OBSTACLE DETECTION BY STEREO VISION, INTRODUCING THE PQ METHOD

H. J. Andersen, K. Kirk, T. L. Dideriksen, C. Madsen and M. B. Holte
Computer Vision and Media Technology Laboratory
Aalborg University, Denmark

T. Bak
Danish Agricultural Sciences
Denmark

Keywords: Computer vision, Autonomous mobile robot, Obstacle detection, Stereo vision.

Abstract: Safe, robust operation of an autonomous vehicle in cross-country environments relies on sensing of the surroundings. Thanks to the reduced cost of vision hardware, and increasing computational power, computer vision has become an attractive alternative for this task. This paper concentrates on the use of stereo vision for obstacles detection in cross-country environments where the ground surface can not be modeled as ramps, i.e. linear patches. Given a 3D reconstruction of the surrounding environment, obstacles are detected using the concept of compatible points. The concept classify points as obstacles if they fall within the volume of cone located with its apex at the point being evaluated. The cone may be adjusted adjusted according the physical parameters of the vehicle. The paper introduces a novel Projection and Quantification method that based on vehicle orientation rotates the 3D information onto an intuitive two dimensional surface plot and quantifies the information into bins adjusted to the specific application. In this way the search space for compatible points is significantly reduced. The new method is evaluated for a specific robotic application and the results are compared to previous results on a number of typical scenarios. Combined with an intuitive representation of obstacles in a two dimensional surface plot, the results indicate a significant reduction in the computational complexity for relevant scenarios.

1 INTRODUCTION

Robotics, control, and sensing technology are today at a level, where it becomes interesting to investigate the development of mobile autonomous vehicles to off-road equipment domains, such as agriculture (Stentz et al., 2002; Bak and Jakobsen, 2004), lawn and turf grass (Roth and Batavia, 2002), and construction (Kochan, 2000). Efficient deployment of such vehicles would allow simple, yet boring, tasks to be automated, replacing conventional machines with novel systems which rely on the perception and intelligence of machines.

One of the most challenging aspects of cross-country autonomous operation is perception such as in agricultural fields, small dirt roads and terrain covered by vegetation. In cases localization may be achieved using technology such as GPS, and paths planned a priori or according to specific application structures, the ability to perceive, or sense, the surrounding environment is essential to driving and thus to the deployment of autonomous vehicles. The perception can be performed by radio, acoustic, magnetic, and tactile sensors. These active sensors or a combination thereof can measure obstacles (Langer et al., 1999; Borenstein and Koren, 1998); however, thanks to the reduced cost of image acquisition devices and to the increasing computational power of computer systems, computer vision has recently become a popular method for sensing the surrounding environment. In comparison with active sensors, computer vision does not interfere when several vehicles are moving simultaneously in the same environment, thereby providing more flexibility and a less expensive solution. On the other hand, computer vision is a computationally complex process, and there are problems intrinsic to the outdoor environment, such as lighting and dynamic range effects, which causes false positives and false negatives.

Here the focus is on obstacle detection using three-dimensional information from a binocular stereo vision system. Stereo images are acquired simultaneously from different points of view, and we search for objects which can obstruct the path of a vehicle. The problem is reduced to identifying the free space (the area into which the vehicle can move safely).

J. Andersen H., Kirk K., L. Dideriksen T., Madsen C., B. Holte M. and Bak T. (2005).
OBSTACLE DETECTION BY STEREO VISION, INTRODUCING THE PQ METHOD.
In *Proceedings of the Second International Conference on Informatics in Control, Automation and Robotics - Robotics and Automation*, pages 250-257
DOI: 10.5220/0001168602500257

The development of the obstacle detection algorithm has been guided by application to the agricultural application domain. While the environment in developed agriculture is semi-structured and well maintained, there may be regions (obstacles), which vehicles should not move into. Obstacles depend on vehicle capabilities and include humans, trees, big rocks, ditches, and other depressions (potentially filled with water). As result it is not feasible to rely on horopter based methods (Badal et al., 1994; Se and Brady, 1998).

This paper first outlines the background in terms of stereo vision and introduces obstacle detection using the concept of compatible points. Next, a novel projection and quantification method is introduced which projects the 3D reconstructed point cloud onto a global ground plane and quantifies the projected the points into bins. In Section 3, the novel method is evaluated by a comparative study with the recently introduced obstacle detection in (Manduchi et al., 2005). The complexities of the algorithms are compared and noise suppression discussed. Finally, the results are discussed and conclusions given.

2 MATERIAL AND METHOD

2.1 Stereo Vision

Three-dimensional information may be acquired in many different ways. However, in this study we will concentrate on the use of binocular stereo, i.e., two cameras giving a right and a left image. In the following, it will be assumed that the cameras used are internally and externally calibrated. Internal camera parameters include focal length, center pixel position, and geometric distortion. External parameters describe the positions and orientations of the cameras.

The key to success in stereo vision is to find matching elements in our stereo pair of images. The elements may be lines, edges, etc., in feature-based matching, or pixels as in area based-matching. The problem is to find the element in the right image which has the highest similarity to an element in the left image.

The search space for matching image elements is limited considerably by the epipolar constraint. This constraint exploits that, given a point in one image, the corresponding point in the second image will always lie on a line, called the epipolar line. Assuming a pinhole camera model, the epipolar line is the projection on the second image plane of the line spanned by the image point and the focal point of the first camera (Trucco and Verri, 1998).

The epipolar constraint reduces the correspondence search space from two dimensions (the whole image) to one dimension (a single line). However, the search may be eased further by rectifying the stereo images before the search. Rectification consists of transforming the images to appear as if they were obtained with parallel cameras with equal focal lengths (Fusiello et al., 1997). After rectification, the epipolar lines become horizontal, so that all corresponding pairs of image elements lie on the same image rows.

From the two rectified images the disparity d may be calculated as the horizontal displacement between the reference pixel in the left image and the candidate pixel in the right image, that is, $x_r = x_l + d$. (Fig. 1). Due to the geometry of parallel axes, decreases with increasing depth.

From the disparity map, the 3-dimensional reconstruction of the scene may be determined by triangulation. Ideally, the two rays from the left and right images should cross a in point. However, due to the quantification in the imaging process this is seldom the case. Hence, the method of triangulation with non-intersecting rays (Trucco and Verri, 1998) is used for the reconstruction.

2.2 Compatible Points and Obstacle Detection

Below, the concept of compatible points, as introduced by (Manduchi et al., 2005), will be presented. The concept addresses the problem that in cross-country environments the ground surface can seldom be modelled as ramps, i.e linear patches. Obstacles in terms of two distinct points in space are defined as follows:

Definition 1
Two 3D points $\mathbf{p_1}$ and $\mathbf{p_2}$ are called compatible with one another if the following two condition are met:

1. Their difference in height is larger than H_{min} but smaller than H_{max}.

$$H_{min} < |p_{2,y} - p_{1,y}| < H_{max}$$

2. The lines joining them form an angle with the horizontal plane larger than θ_{max}.

$$\frac{|p_{2,y} - p_{1,y}|}{\|\mathbf{p_2} - \mathbf{p_1}\|} > \sin\theta_{max}$$

Definition 2
Two 3D points, $\mathbf{p_1}$ and $\mathbf{p_2}$, are defined as belonging to the same obstacle if one of the following two conditions are met:

1. The 3D points, $\mathbf{p_1}$ and $\mathbf{p_2}$, are compatible.
2. A chain of compatible point pairs linking $\mathbf{p_1}$ and $\mathbf{p_2}$ exists.

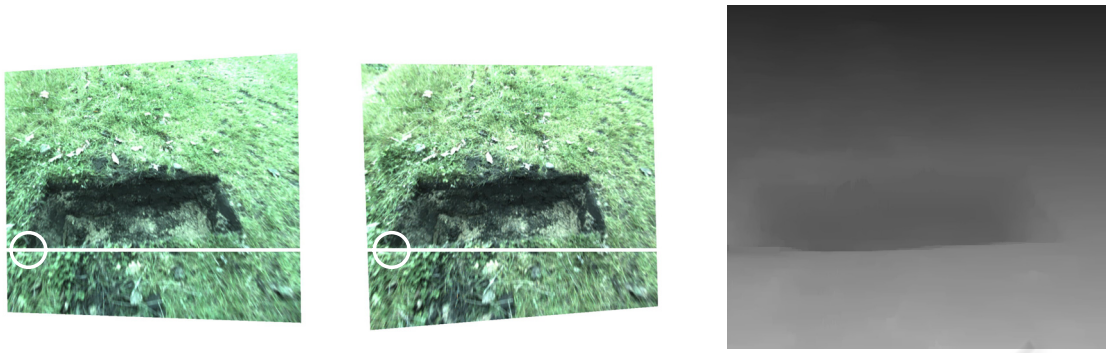

(a) Left rectified image. (b) Right rectified image. (c) The disparity map.

Figure 1: Calculation of disparity for a hole in a grass lawn, i.e. a concave obstacle. The white lines indicates the epipolar lines in the two images. The objective is to find the pixel in the right image with the highest similarity to the pixel in left image, illustrated with white circles. The disparity is the displacement between the two pixels.

The two definitions translate, for a given point $\mathbf{p}$, into a volume of two symmetrical truncated cones in 3D space, with apexes placed in $\mathbf{p}$. Points located inside the volume are compatible with the given point $\mathbf{p}$, figure 2.

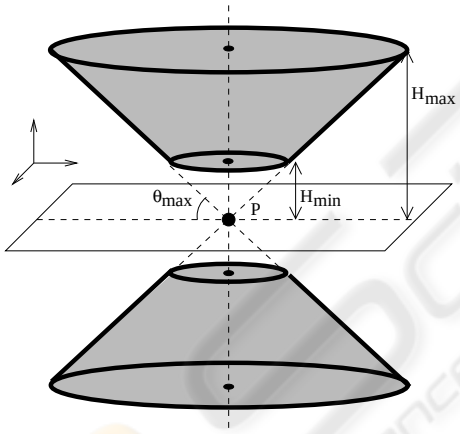

Figure 2: Geometric interpretation of the parameters H_{min}, H_{max} and θ_{max}.

According to definition 1 and 2, the size and shape of the cone volume depends on the variables H_{min}, H_{max} and θ_{max}. These parameters may all be related to the physical dimension of a specific vehicle. H_{max} states the height at which it is able to drive under and/or the distance at which it can pass between two obstacles. H_{min} defines the height of undulations in the surface which the vehicle can easily pass, and θ_{max} the slope rate it is able to climb.

Manduchi et al. 2005 suggested two methods for detection of obstacles based on the compatible point concept, respectively, OD1 and OD2. In OD1, both the upper and lower cone at a given point are considered whereas for the OD2 method only the upper cone is considered for classification of points. The two approaches reach the same result and in the following only OD2 will be used. Figure 3 illustrates the principle in a synthetic scene with four compatible points.

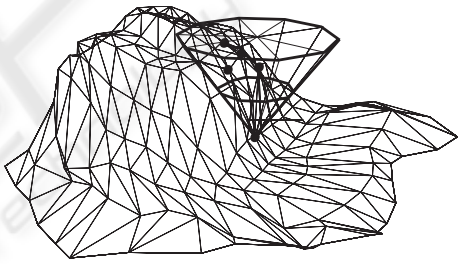

Figure 3: Classifications of obstacle points by the compatible points method (vertex are the reconstructed points). The cone apex is placed in the point being evaluated. The four points which falls inside the cone together with the point being evaluated are all classified as obstacle points.

A computational yet expensive part of the algorithm is the search for 3D points located inside the truncated cone. A naive implementation would be to search through all 3D points, evaluating each one. To reduce the search space Manduchi et. al propose a method for limitation of the search space by projection of the truncated cones onto the disparity map, as illustrated in figure 4. For projection, the width and height of the triangles b and h as illustrated in figure 4, are determined by:.

$$h = \frac{H_{max} f}{p_z} \quad b = 2\left(\frac{H_{max} f}{p_z} \frac{1}{\tan\theta_{max} \cos v}\right) \quad (1)$$

Where f is the focal length of the camera, p_z is the z coordinate of the point and v is the azimuth angle. As a result, the search may be limited to 3D points

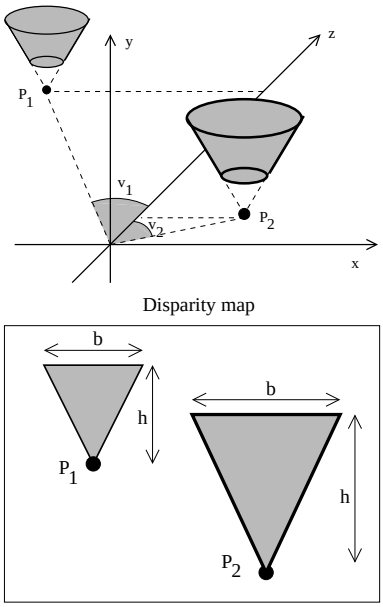

Figure 4: Reducing the 3D search space by projection of the cones onto the disparity map. Top truncated cones in 3D. Bottom their projection onto the disparity map

included in the projected truncated cones in the disparity map. However, eq. 1 is only valid in the ideal case, where the vehicle does not pitch or roll. In order to compensate for this Manduchi et. al. introduced a pitch compensation factor, α, by:

$$\alpha = \frac{1}{\cos\gamma \pm \frac{H_{max}}{p_z}\sin\gamma} \qquad (2)$$

Where γ is the immediate pitch angle. The resulting triangle is adjusted by multiplication of h with α, Vehicle roll is simply compensated by an expansion of the triangle by addition of a factor to both b and h.

2.3 Introducing the PQ method

Below, the new method *Projection and Quantification, PQ* for representation of the three-dimensional point cloud from the reconstructed scene will be introduced. The method operates on the counter rotated point cloud ($\mathbf{P_{cr}}$) according to the robots pitch (R_{pitch}) and roll (R_{roll}) and the default orientation of the stereo setup ($R_{default}$), by:

$$\mathbf{P_{cr}} = (R_{pitch}R_{roll}R_{defualt})\mathbf{P} \qquad (3)$$

where $\mathbf{P}$ is a matrix $3 \times m$ gathering all the reconstructed points (m = number of points), and R_* rotation matrices. After the counter rotation, the method consists of the following two steps:

P - step which Project the counter rotated 3D point cloud onto the XZ-plane, (i.e. the global ground plane)

Q - step which Quantify the projected point cloud into predefined bins on the XZ-plane

The counter rotated and quantified point cloud may be regarding as a two dimensional surface plot. This will be denoted as the PQ-representation. A bin may contain several points. Further, the quantification may be adjusted to the specific application i.e. the size of the robot and/or size of the obstacles. A fine quantification will make it possible to detect small obstacles whereas a coarser one will increase the operational speed. For representation of the points quantified into a specific bin, several metrics may be used as: the mean, max, min, median etc. In this study, the median value of the points quantified into a given bin will be used as a representation of its estimated height. The median value is chosen due to its capabilities of suppressing salt and pepper noise, which is likely to occur in 3-dimensional reconstructions. The PQ-representation of the images in figure 1, is shown in figure 5.

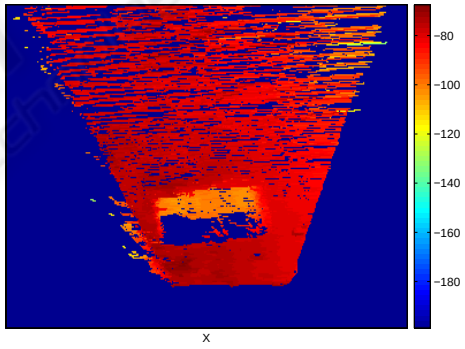

Figure 5: The PQ representation of the images in figure 1.The bins are represented by their median values in cm as the distance from the camera setup. Dark blue bins are empty. The hole in the lawn is app. 120 cm broad, 30 cm wide and 25 cm deep. The bin size is 1 cm x 1 cm at ground surface. The color bar indicates distance from the cameras, n.b. dark blue areas is occluded or not within the field of view.

As the point cloud is counter rotated the projection of the truncated cones onto the PQ-representation is straight forward. In the counter rotated point cloud the center axis of the cone becomes perpendicular to the XZ-plane and hence it may be discretized according to the quantification of the PQ-representation, as illustrated in figure 6.

As a result, detection of compatible points may be done simply by evaluating whether the median value

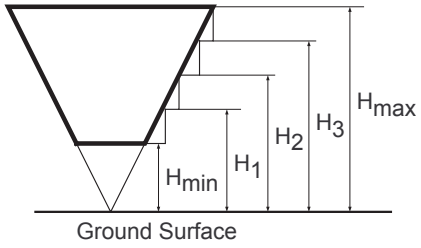

Figure 6: Side view of the discretized truncated cone. H_{min} indicates the minimum value of a bin before it is classified as an obstacle point. H_1, H_2, and H_3 is the lower limit values for when a point is not classified as an obstacle, i.e. the value increases as we move away from the apex according θ_{max}. All bins with a value bigger than H_{max} is not classified as obstacles.

of a bin is bigger than the lower limited of the discrete truncated cone, i.e. greater than H_{min}, H_1, H_2, H_3 in figure 6, and lower that the maximum limit H_{max}, i.e the top of the cone.

3 COMPARING THE PQ AND OD2 METHODS

The following section will present a comparative study of the PQ and OD2 methods. The unbound complexity of the two methods will be evaluated. However, when working with computer vision methods the unbound complexity is not that interesting from a practical point of view, as the image dimensions give a very concrete bound for complexity of the methods. Hence a more concrete comparison will be investigated according to a specific robot.

3.1 Robot setup

For the comparison of the two methods the autonomous platform (Bak and Jakobsen, 2004), will be used (figure 7). From the physical dimensions of the robot the setting of the parameters for the OD2 and PQ methods may be determined. Table 1 summarizes the values used in the following simulations and experimental work.

The cameras in the stereo setup were mounted at a height of 75 cm and had a base-line of 16.4 cm, which gave an uncertainty in depth of 1.84 cm at a distance of 1.06 m along the optical axis. The image field of view covered an area from the front wheels to app. 150 cm in front of the robot and was app. 140 cm wide in the center of the image field.

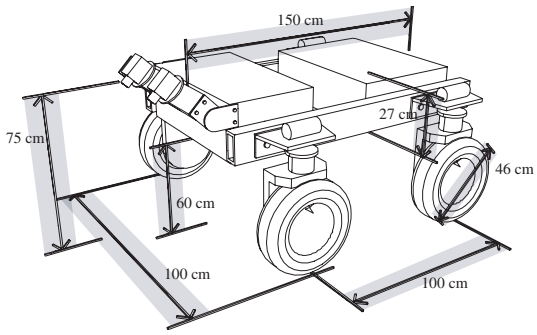

Figure 7: The physical dimensions of the API robot.

Table 1: Parameters used in the comparative study.

Parameter	Value
H_{min}	10 cm
H_{max}	121 cm
θ_{max}	60°
Camera tilt angle	45°
Image resolution	1280×1024
PQ quantization	1 cm $\times$ 1 cm

3.2 Worst case Complexity

For the OD2 method, a triangle is imposed in the disparity image for all pixels. Further, depending on the resolution of the disparity map, a fraction a of the image pixels shall be compared with the pixels inside the projected triangle. This gives a worst case complexity of $O(n^2)$:

$$n(c + n\frac{1}{a}) \tag{4}$$

where c denotes the constant for projection of the triangles and a the fraction of pixels inside the projected truncated cone.

For the PQ method, all 3D reconstructed points are first counter rotated and projected onto the XZ-plane. After this operation, a fraction of the bins depending on the quantification of the XZ-plane must be compared with one another. This also gives a worst case complexity of $O(n^2)$:

$$n(d + n\frac{1}{b}) \tag{5}$$

where d denotes the constant for the counter rotation and projection of the 3D reconstructed points and b the fraction of bins which has to be compared.

3.3 Bounded Complexity

For illustration of the two methods, operational characteristics three different scenarios are simulated (figure 8). A flat surface (plan lawn), a vertical obstacle

(a wall), and a landscape with cone obstacles (trees). The simulations clearly illustrate the main difference between the two methods. For the OD2 method, the whole disparity has to be searched in all three simulations, whereas for the PQ method the search space is limited to include only the bins with points projected into them. This gives a severe reduction in the search space for the vertical obstacle, where the area in black may be excluded. Also, the size of the squares are unaffected by the location in the PQ-representation compared to the imposed triangles for the OD2 that in the worst case almost span the whole disparity map, i.e figure 8.

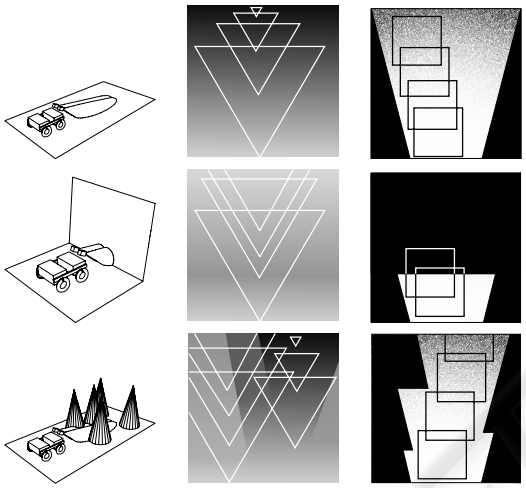

Figure 8: Illustration of the search space reduction for the OD2 and PQ methods for the API robot. 1st column, illustration of different scenarios. Top row, flat surface scenario. Middle row, vertical obstacle. Bottom row, cone obstacles. 2nd column, the disparity map with triangles imposed illustrating the span from the largest to the smallest search space reduction. 3rd column, the PQ-representation with squares illustrating the reduction of the search space.

For a more quantitative comparison of the bounded complexity the, two methods were evaluated by simulating the rotation of a planar surface in front of the robot (figure 9). The angle by V was varied from from 0 to 90 degrees in steps of 5 degrees. At each step the number of comparison for the two methods was logged.

The result of the simulation is plotted in figure 11. The figure clearly illustrates the characteristics of the two methods. The PQ method has its worst performance at an angle of 0 degree with increasing number of comparisons until 90 degrees. For the OD2 method, the characteristics are just the opposite. This method has the lowest number of comparisons at 90 degrees with increasing number of comparisons till 0 degrees is reached. However, at all angles the PQ method is significantly better than the OD2 method, ranging from a factor of 44 at 0 degrees and 270 at 90 degrees.

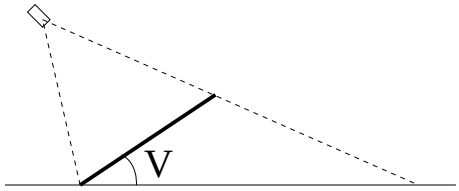

Figure 9: The ground surface used in the simulated comparison.

3.3.1 Noise suppression

In order to evaluate the PQ noise suppression, the robot traveled across a flat gras lawn. For estimation of the disparity map the method in (Birchfield and Tomasi, 1999), was used. Five pairs of stereo images were captured. In all cases the undulations in the surface were not exceeding that of H_{min} threshold of 10 cm, so pixels classified as obstacles may have been regarded as being due to faults in the disparity estimation. An example of the scenario is illustrated in figure 10.

Table 2: Noise suppression. Points denotes the number of data points addressed and %-Faults the percentage of points incorrect classified as obstacles. For the OD2 method this correspond to all image pixels, i.e. 1280×1024 equals 687219, whereas for the PQ method there is a reduction in the points to process due to the quantification.

PQ		OD2	
Points	%-Faults	Points	%-Faults
48014	2.6	687219	11.9
47514	3.5	687219	13.0
46478	4.3	687219	12.2
45260	7.0	687219	24.7
45157	17.5	687219	37.3
In average:			
46485	6.9	687219	19.8

Table 2 summarize the result of the noise suppression evaluation. First, as with the bounded complexity, the impact of the quantification in the PQ method reduces in average the necessary points to process by a factor 15. Further, the median representation of the bin values reduces the percentage of incorrect classified points by approximately a factor 3.

4 DISCUSSION

A new method for representation of the reconstructed 3D points cloud from a binocular stereo vision sys-

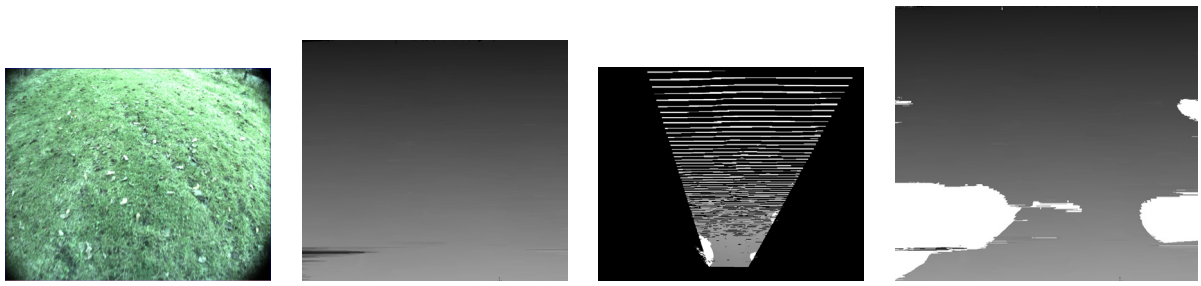

a b c d

Figure 10: Noise suppression capabilities of the PQ and OD 2 methods. a) Left image of a flat grass lawn. b) Disparity map. c) PQ representation, white areas are incorrectly classified as obstacles. d) Results of the OD2 method white areas are incorrectly classified as obstacles.

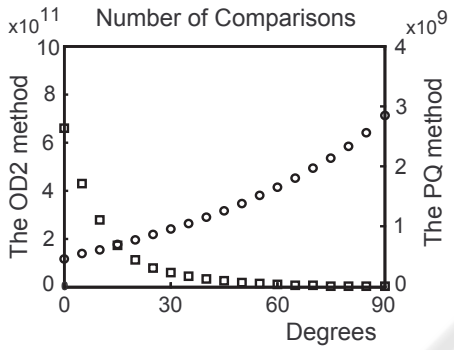

Figure 11: Number of comparison for OD2 and PQ methods when a flat ground surface is rotated in front of the robot, as illustrated in figure 9. The OD2 method is illustrated with a circle and the PQ with a square. Notice the difference in the magnitude of the two y-axis.

tem is presented. For evaluation of the method it is compared to the recently introduced OD2 method by (Manduchi et al., 2005). In the evaluation problems regarding occluded areas has not been addressed. However, in terms of computational demand occluded areas will have the same impact on the two methods. The question is more how these shall be classified. A conservative approach is to regard all occluded areas as obstacles areas, i.e. the robot shall not move into these.

The comparative study has in this study been based a specific robotic platform. Whether this platform favor one of the method is not evaluated. However the physical dimension of the robot and the mounting of the stereo setup may be regraded as being very realistic for a cross-country operating robot.

More critical is the evaluation of the noise suppression. This study is more an evaluation of what may be called the implicit noise suppression of the PQ-method. Clearly, the performance of the OD2-method may be improved by median or other filtering techniques of the disparity map. However, these method will also increase the performance of the PQ-method. Hence these results shall only been seen as an example of the implicit noise suppression due to the median representation of the bin values in the PQ-representation.

5 CONCLUSION

This paper addressed the problem of identifying obstacles for an autonomous vehicle operating in a cross-country domain. A novel algorithm was presented based on previous results from (Manduchi et al., 2005). The new Projection and Quantification method projects the 3D information from a stereo vision system into the surface plane in front of the robot and quantifies the depth information into bins that may be adjusted to the specific application. The bins allow quantification of a cone representing terrain that should not be traversed by the vehicle and represents both positive and negative obstacles typically encountered in cross-country environments. The new algorithm simplifies the computation compared to (Manduchi et al., 2005) for a number of specific scenarios. The result is a modified algorithm (the PQ method), that provides an intuitive representation of the surrounding environment and simple detection of obstacles.

REFERENCES

Badal, S., S. Ravela, S., Draper, B., and Hanson, A. (1994). A practical obstacle detection and avoidance system. In *2nd IEEE Workshop on Applications of Computer Vision*, pages 97–104.

Bak, T. and Jakobsen, H. (2004). Agricultural robotic plat-

form with four wheel steering for weed detection. *Biosystems Engineering*, 87(2):125–136.

Birchfield, S. and Tomasi, C. (1999). Depth discontinuities by pixel-to-pixel stereo. *International Journal of Computer Vision*, 35(3):269–293.

Borenstein, J. and Koren, Y. (1998). Obstacle avoidance with ultrasonic sensors. *IEEE Journal of Robotics and Automation*, 4(2):213–218.

Fusiello, A., Trucco, E., and Verri, A. (1997). Rectification with unconstrained stereo geometry. In *Proceeding of the British Machine Vision Conference*, pages 400–409.

Kochan, A. (2000). Robots for automating construction - an abundance of research. *The Industrial Robot*, 27(2):111–113.

Langer, D., Mettenleiter, M., Hartl, F., and Frohlich, C. (1999). Imaging laser radar for 3-d surveying and cad modelling of real world environments. In *Proceedings of the International Conference on Field and Service Robotics*, pages 13–18.

Manduchi, R., Castano, A., Talukder, A., and Matthies, L. (2005). Obstacle detection and terrain classification for autonomous off-road navigation. *Autonomous Robots*, 18:81–102.

Roth, S. A. and Batavia, P. (2002). Evaluating path tracker performance for outdoor mobile robots. In *Automation Technology for Off-Road Equipment*.

Se, S. and Brady, M. (1998). Stereo vision-based obstacle detection for partially sighted people. In *Proceedings of Third Asian Conference on Computer Vision ACCV'98*, pages 152–159.

Stentz, A. T., Dima, C., Wellington, C., Herman, H., and Stager, D. (2002). A system for semi-autonomous tractor operations. *Autonomous Robots*, 13(1):87–103.

Trucco, E. and Verri, A. (1998). *Introductory Techniques for 3-D Computer Vision*. Prentice Hall.